GENERATION OF SPECTRUM COMPATIBLE TIME HISTORIES FOR BUILDING DESIGN BY AN EMPIRICAL METHOD USING MEGATHRUST EARTHQUAKE SCENARIOS

Armando Sifuentes[*] **Supervisor: Izuru OKAWA**[**]
MEE12607

ABSTRACT

An empirical method is used to simulate spectrum compatible time histories for a megathrust earthquake scenario in Peru. The Pisco earthquake (Mw 8.0) is the earthquake scenario. An empirical attenuation formula for acceleration response spectra provides the target spectrum. Moreover, empirical formulas to evaluate the mean μ_{tgr} and the variance σ_{tgr}^2 of group delay time are used. The empirical formulas use site coefficients to represent local characteristics of ground motions due to underlying soil structure. Deep shear-wave velocity profiles in Lima, Peru and soil profile information from the KiK-net seismic network in Japan are used to calculate transfer functions and evaluate the site effect. Although there is good agreement with response spectra in a certain range of periods and peak acceleration values in time domain for observed and simulated ground motions, it is not advisable the direct use of empirical formulas. However, the procedure to construct waveforms, based on the phase content, used has proven to be a good technique to simulate ground motions.

Keywords: Lima city, Pisco earthquake, spectrum compatible time history, group delay time, transfer function.

1. INTRODUCTION

1.1. Background

Peru and Japan are both located in the "Ring of Fire", an area where about 90% of the total number of earthquakes in the world occurs (USGS, 2012). As a part of actions taken to aim for disaster risk reduction, the design and construction of safety infrastructure must be taken into consideration and a performance evaluation must be conducted if required. Thus, it is necessary to use a design ground motion expressed as a time history when performing nonlinear dynamic analysis, usually applied to high-rise and base-isolated buildings. In this study, to achieve the time history generation for building design using Peru earthquake scenarios, the empirical method proposed by Satoh et al. (2010) is used.

1.2. Objectives

The objective of this study is the use of an empirical method to simulate earthquake ground motions to be used in building design for a megathrust earthquake scenario in Peru and to compare the results with observed recorded ground motions. The method uses empirical formulas developed with recorded ground motions in Japan. Therefore, the possibility of the use of these empirical formulas to characterize earthquake ground motions in Peru, to overcome the lack of these formulas, will be evaluated.

[*]Japan-Peru Center for Earthquake Engineering Research and Disaster Mitigation (CISMID), Lima, Peru
[**]BRI Chief Fellow, Building Research Institute (BRI), Tsukuba, Japan.

2. DATA

2.1. Empirical Formulas

Empirical formulas used in this study were proposed by Satoh et al. (2012). These formulas were proposed as a method for evaluating the long-period ground motion time history with periods from 0.1 to 10 s using earthquake magnitude, shortest distance to the source area and location of the hypocenter.

3. METHOD

3.1. Spectrum Compatible Time History

Spectrum compatibles time histories are time histories with their response spectrum consistent with a target spectrum. This target spectrum could be referred to as a design spectrum, uniform hazard spectrum or any other that represents buildings responses including the characteristics of the site where the analysis is being carried out.

3.2. Target Spectrum

An empirical formula for the Pacific plate events is used to define the target spectrum. This formula relates the 5% damping acceleration response spectra $S_a(T)$ with the moment magnitude and the shortest distance from recording station to the assigned source area of each recorded event. Acceleration values of response spectra are expressed by

$$\log_{10} S_a(T) = a_1(T)M_W + a_2(T)M_W^2 + be(T)R - \log_{10}\left(R^{p(T)} + d(T)10^{0.5M_w}\right) + c_0(T) + c_j(T)\,, \quad (1)$$

where, T is period in seconds. M_W is moment magnitude and R is shortest distance from the recording site to the coseismic rupture in kilometer, and $a_1(T)$, $a_2(T)$, $be(T)$, $p(T)$, $d(T)$, $c_0(T)$, $c_j(T)$ are coefficients determined with the least squares analysis. $a_1(T)$ and $a_2(T)$ are the coefficients representing the source properties. $be(T)$ represents the property for propagation from the Pacific plate. The coefficient $c_0(T)$ is assumed to be the site amplification factor for the KiK-net FKSH19 station which is regarded as the benchmark station on the seismic bedrock and, $c_j(T)$ is the site coefficients for the j-th recording station

3.3. Mean and Variance of Narrow-band Group Delay Time

The mean value μ_{tgr} of group delay time corresponds to an average arriving time of wave group in a narrowband and the standard deviation σ_{tgr} of group delay time corresponds to the scatter of the arriving time that is the duration time of the wave group in a narrowband (Satoh et al., 2010).

The mean μ_{tgr} and the variance σ_{tgr}^2 of group delay are expressed by the following empirical formulas

$$\mu_{tgr}(f) = A_{1tgr}(f)M_0^{1/3} + Be_1(f)X + C_{1j}(f)\,, \quad (2)$$

$$\sigma_{tgr}^2(f) = A_{2tgr}(f)M_0^{1/3} + Be_2(f)X + C_{2j}(f)\,, \quad (3)$$

where, M_0 is seismic moment in dyne-cm (10^{-7} N-m), X is hypocentral distance in kilometer, f is frequency. A_{1tgr}, Be_1, C_{1j}, A_{2tgr}, Be_2 and C_{2j} are coefficients determined by the least squares analysis. The inverse of Be_1 indicates the propagation velocity of seismic waves radiated from the seismic sources from the Pacific plate. C_{1j} and C_{2j} are called site coefficients.

3.4. Generation of Waveform

Satoh et al. (1996) explained fundamental formulation of group delay time based on the relation between group delay time $tgr(\omega)$ and the phase angle shown in Eq. (4) (Papoulis, 1962) , written as

$$tgr(\omega) = \frac{d\varphi(\omega)}{d\omega}, \tag{4}$$

where, ω is circular frequency and $\varphi(\omega)$ is Fourier phase angle.

Therefore, since group delay time is the first derivative of the Fourier phase angles with frequency, once the initial phase angle is fixed and random numbers are given, the other phase angles are recursively calculated using a normal distribution with the mean μ_{tgr} and standard deviation σ_{tgr} (Satoh et al., 2010). Finally, it is possible to construct a Fourier phase spectrum that combined with an assumed Fourier amplitude spectrum generates a waveform applying the Inverse Fourier Transform. The Fourier amplitude spectrum must be iteratively changed to match the target spectrum.

4. PERU CASE

4.1. Earthquake Scenario

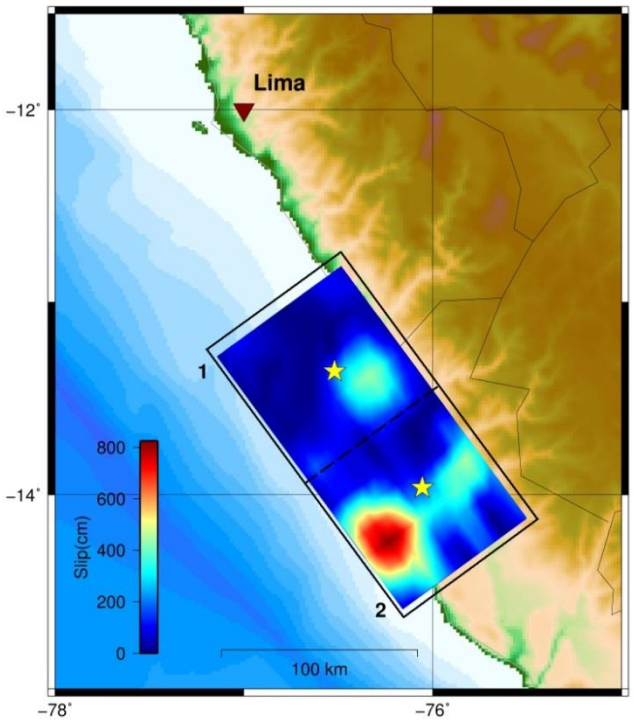

Figure 1. Surface projection of slip distribution and source division (dashed line). Epicenters for each segment are indicated by yellow stars.

The August 15, 2007 Pisco earthquake is used as the earthquake scenario. This earthquake had a moment magnitude Mw of 8.0 (USGS, Harvard CMT). The hypocenter was located at 13.354S and 76.509W, at a depth of 39 km (USGS) in central Peru, offshore of the city of Pisco. Source models for this earthquake favor the existence of two subevents (Ji and Zeng, report, 2007; Sladen, 2010) about 60 s apart, i.e., slip on the second event started 60 s after slip initiated on the first event.

To simulate adequately two events, it is indispensable to divide the source area into two, each one characterized by values of seismic moment and moment magnitude. For this purpose, slip distribution information for each subevent of the source model proposed by Ji and Zeng (2007) and rigidity values calculated using information from the global crustal model CRUST 2.0 (Bassin et al. 2000) are used. The following equation describes how to calculate seismic moment m_0 for each segment:

$$m_0 = \sum_{i=1}^{n} \mu_i \times D_i \times S_i, \tag{5}$$

where, for each subfault i, μ_i is rigidity, D_i is slip and S_i is area; and n is the number of subfaults for each segment.

Figure 1 shows the surface projection of slip distribution, epicenter and geometry of the two segments into which the source area was divided. Moment magnitude M_w is obtained using seismic moment M_0 and the following equation (adapted from Hanks and Kanamori, 1979)

$$M_w = \frac{14}{3} \log M_0 - 10.7 \,, \tag{6}$$

where the seismic moment M_0 is in N-m.

The seismic moment in N-m for the first and second segment is 0.6104E+21 and 1.2718E+21, respectively. The moment magnitude M_w for the first and second segment is 7.8 and 8.0, respectively. The epicenter for the first segment is the same as the epicenter given for USGS. The epicenter for the second segment is obtained based on the time between ruptures and the source model proposed by Ji and Zeng (2007).

4.2. Choice of Site Amplification Factors

To use empirical equations correctly it is important to define appropriate values of site coefficients that represent local characteristics of ground motions due to soil structure for soils in Japan and used them to represent soil behavior in Lima, Peru.

CAL, CSM, PQR and VSV profiles in Lima, Peru from Calderon (2012) are used. CAL, CSM and VSV profiles correspond to CISMID accelerometer network (www.cismid-uni.org/redacis/) stations with the same name. PQR profile and the CDL-CIP station differ in their locations even though they are located in an area with the same type of soil (CISMID, 2005). Quispe (2010) presented a shear-wave velocity profile for shallow soil structure of the CDL-CIP station; however, PQR profile is used since it provides information for deeper soil structure. The VSV station had not been deployed during the Pisco earthquake and VSV profile is used to evaluate how the ground motion had been in this location. In Japan, the KiK-net seismic network (http://www.kyoshin.bosai.go.jp/) provides the soil structure information of locations where its stations are deployed.

Thus, site effect is evaluated using transfer functions to compare soils in Lima, Peru and Japan. It is found that the CAL station in Lima exhibited similar behavior to the FKSH11 and MYGH02 stations in Japan as shown in Figure 2(a) and (b). In addition, the CSM station showed similar behavior to the FKSH17 and IWTH21 stations (see Figure 2(d) and (e)), the CDL-CIP station to the FKSH02 and FKSH16 stations, and the VSV station to the IWTH24 station.

5. RESULTS

Figure 2(c) and (f) show response spectra for observed ground motion and simulated ground motions for the Pisco earthquake using selected site coefficients (c_j, C_{1j} and C_{2j} in Eq. (1), (2) and (3), respectively) at stations CAL and CSM, respectively. Response spectra of simulated ground motions are the arithmetic average of ground motions generated using six sets of random numbers.

The response spectra of simulated ground motions exhibited in most of the cases coincidences of the interval of period where maximum acceleration values were observed for observed ground motion. However, values of acceleration differ due to different levels of amplification between selected station in Lima and Japan. The response spectra of simulated ground motion at the VSV station showed acceleration values greater than 300.0 cm/s^2 for periods less than 0.6 s.

Figures 3 shows simulated ground motions for stations CAL and CSM using different sets of random numbers. Simulated ground motions are compared with observed recorded ground motions for stations CAL and CSM.

There is a good agreement between amplitudes of observed and simulated ground motions for the two subevents. The duration of simulated ground motions in most of the cases is less than the duration of observed ground motions at each station. Simulated ground motions at the VSV

station present peak acceleration values near 120.0 cm/s^2 with evident long period content. Amplitudes for the two subevents do not differ significantly. However, as the observed ground motions in different stations the peak acceleration values of the simulated ground motions for the first subevent are less than for the second subevent for most of the sets of random numbers.

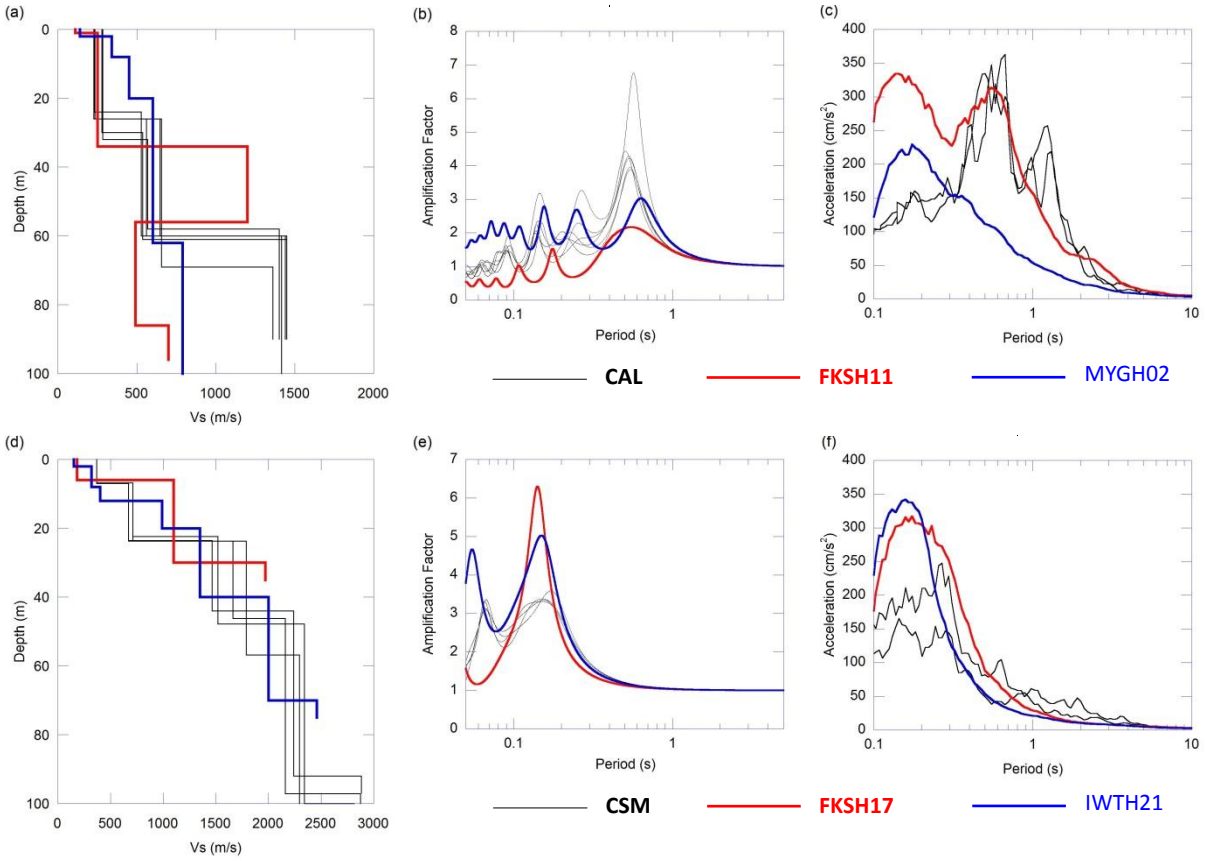

Figure 2. CAL, FKSH11 and MYGH02 (a) shear-wave velocity profiles and (b) transfer functions. (c) Response spectra of observed ground motion and generated ground motions at the CAL stations. CSM, FKSH17 and IWTH21 (d) shear-wave velocity profiles and (e) transfer functions. (f) Response spectra of observed ground motion and generated ground motions at the CAL stations.

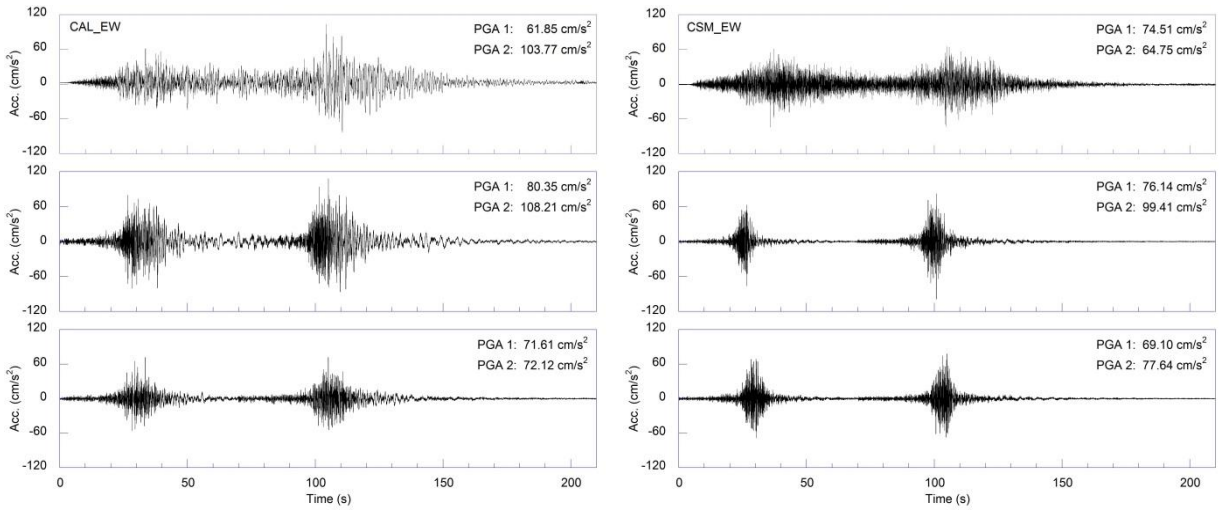

Figure 3. Observed and generated ground motions at stations CAL and CSM.

6. CONCLUSIONS

Although there is good agreement with response spectra in a certain range of periods and peak acceleration values in time domain for observed and simulated ground motions, it is not advisable the direct use of empirical formulas to characterize ground motions in Peru. Site coefficients in empirical formulas were used to estimate a similar behavior of soils in Lima, Peru and may not represent overall site conditions. However, the procedure to construct waveforms used in this study, based on phase angle characteristics and their relation with the mean and standard deviation of group delay time in earthquake ground motions, has proven to be a good technique to simulate ground motions. Therefore, efforts must be made to developed empirical formulas to characterize earthquake ground motions in Peru. This involves tasks as the enhancement of strong ground motion observation to obtain the necessary data.

ACKNOWLEDGEMENTS

I would like to express my gratitude to Dr. Toshiaki YOKOI -International Institute of Seismology and Earthquake Engineering- for his valuable advice, guidance and support during the time this study was carried out.

In this study, strong motion records and soil profile information from KiK-net seismic network of the National Research Institute for Earth Science and Disaster Prevention (NIED) were used. In addition, The Generic Mapping Tools (GMT) was used for making maps.

REFERENCES

Bassin, C., Laske, G. and Masters, G., 2000, EOS Trans AGU, 81, F897.
Calderon, D., 2012, Graduate School of Engineering, Chiba University, Japan.
CISMID, 2005, Universidad Nacional de Ingeniería, Lima, Perú (in Spanish).
Hanks, T. C. and Kanamori, H., 1979, J. Geophys. Res., 84, 2348-2350.
Ji, C. and Zeng Y., 2007, Retrieved July 2013 from http://earthquake.usgs.gov/earthquakes/eqinthenews/2007/us2007gbcv/finite_fault.php
Papoulis, A., 1962, McGRAW-Hill.
Quispe, G., 2010, Master Thesis, National Graduate Institute for Policy Studies, Building Research Institute, Japan, 32p.
Satoh, T., Uetake, T. and Sugawara, Y., 1996, Proceedings. of 11th WCEE, Paper No.149.
Satoh, T., Okawa, I., Nishikawa, T., Sato, T., Seki, M., 2010, J. Struct. Constr. Eng., AIJ, Vol. 75, No. 649, pp. 521-530 (in Japanese).
Satoh, T., Okawa, I., Nishikawa, T., Sato, 2012, J. JAEE, Vol.12, No.4, pp. 354-373 (in Japanese).
Sladen, A., Tavera, H., Simons, M., Avouac, J. P., Konca, A. O., Perfettini, H., Audin, L., Fielding, E. J., Ortega, F. and Cavagnoud, R., 2010, J. Geophys. Res., 115, B02405, doi: 10.1029/2009JB006429.